separations

MDPI

Article

Post-Functionalization of Bromo-Substituted Ether-Linked Polymers via Ullman Coupling Reaction: Synthesis, Characterization and Their Role toward Carbon Dioxide Capture

Tareq M. A. Al-Shboul [1], Suha S. Al-Tarawneh [1,*], Taher S. Ababneh [2] and Taghreed M. A. Jazzazi [2,*]

[1] Department of Chemistry and Chemical Technology, Tafila Technical University, Tafila 66110, Jordan; tareq92@hotmail.com
[2] Department of Chemistry, Yarmouk University, Irbid 21163, Jordan; tababneh@yu.edu.jo
* Correspondence: s.tarawneh@ttu.edu.jo (S.S.A.-T.); taghreed.j@yu.edu.jo (T.M.A.J.)

Abstract: A new open-chain ether-linked polymer has been prepared via nucleophilic aromatic substitution reaction on a C-F bond of 1,4-dibromo-2,5-difluorobenzene by using 2,2-bis(4-hydroxyphenyl) hexafluoropropane (bisphenol AF or BAF). The new polymer (PE-AF) has shown a good solubility in non-polar solvents, good thermal stability (up to 300 °C) and random surface morphology. Tailoring these properties has been achieved by utilizing the post-modification synthetic methodology on the bromo-sites of the polymer backbone via the application of an Ullmann coupling reaction with aniline to form the polymer (PE-Sec-NHPh). The successful synthesis of the polymers has been confirmed by elemental analysis, infrared spectroscopy (IR), ^{1}H- and ^{13}C-NMR and ^{13}C CP-MAS solid state. Upon incorporation of the aniline linker, the nitrogen content increased when compared with the parent polymer chain, and thus PE-Sec-NHPh revealed a higher thermal stability up to 350 °C and a more uniformly aggregated morphology (spherical particles ca. 0.3–0.1 μm). A further evaluation has been conducted on the polymers by measuring their surface tendency toward carbon dioxide capture. Interestingly, despite their non-porous nature, the polymers demonstrated a reasonable amount of gas capture that reached 90.0 and 41.0 mg/g for PE-Sec-NHPh and PE-AF, respectively. Furthermore, the calculated CO_2 binding affinities of the polymers are consistent with data reported previously in the literature.

Keywords: ether-linked polymers; thermal stability; ullmann coupling; surface morphology; CO_2-capture

check for updates

Citation: Al-Shboul, T.M.A.; Al-Tarawneh, S.S.; Ababneh, T.S.; Jazzazi, T.M.A. Post-Functionalization of Bromo-Substituted Ether-Linked Polymers via Ullman Coupling Reaction: Synthesis, Characterization and Their Role toward Carbon Dioxide Capture. *Separations* **2022**, *9*, 55. https://doi.org/10.3390/separations9030055

Academic Editor: Federica Raganati

Received: 15 January 2022
Accepted: 16 February 2022
Published: 23 February 2022

Publisher's Note: MDPI stays neutral with regard to jurisdictional claims in published maps and institutional affiliations.

Copyright: © 2022 by the authors. Licensee MDPI, Basel, Switzerland. This article is an open access article distributed under the terms and conditions of the Creative Commons Attribution (CC BY) license (https://creativecommons.org/licenses/by/4.0/).

1. Introduction

In the advances of polymer research, there has been a pronounced interest in studying the properties and applications of conjugated organic polymers due to their vital usage in catalysis, electronics, solar cells, sensors, drug-delivery and design, as well as in environmental applications [1–3]. This wide range of applications is due to their outstanding properties that include, but are not limited to, good thermal stability, flame retardancy, electrical properties, solvent and oxidative resistance properties, absorption, and feasible processability [4,5]. In this regard, there has been a notable focus on the heteroatoms-containing organic polymers such as polyimines, polythiophene, polybenzimidazole and polyoxazole, where nitrogen, sulfur or oxygen can be found in their structural frameworks [6–8]. The presence of heteroatoms with free-lone pairs of electrons makes these polymers suitable adsorbents for acids via physical interactions or for metal-ion coordination. Such polymers can be synthesized via several methods including polycondensation polymerization, aromatic substitution reactions, catalytic polymerization and pre- and post-functionalizations [9–13].

The growing environmental effects of climate change and global warming, which are primarily caused by increased fossil fuel consumption and associated combustion product emissions, have prompted many researchers to focus their efforts on reducing CO_2 emissions as the primary greenhouse gas contributor in the atmosphere [14–16]. The effects can be mitigated by employing highly effective capture and storage techniques or adopting more environmentally friendly energy sources [17,18]. Among the principal combustion flue gas elements, such as CO_2, SO_2, N_2O and N_2, CO_2 has been shown to be extensively present in the atmosphere, with concentrations now exceeding 400 parts per million [15,16]. Due to its efficacy and low cost, CO_2 capture is currently the most popular method for reducing atmospheric CO_2 accumulation and its harmful impacts [16,19]. Studies have shown that CO_2 can be captured effectively using absorption, adsorption, membrane separation or cryogenic distillation techniques [20–26].

Motivated by the vital properties and applications of polymers, we have adopted two new types of polymers for synthesis. Herein, we report the synthesis of an open chain ether-linked polymer via a nucleophilic aromatic substitution reaction followed by incorporation of a nitrogen atom through a post-functionalization methodology via applying an Ullman coupling reaction [27]. The new polymers have been characterized and compared to ensure the achievement of tailored properties due to the inclusion of nitrogen content besides the presence of the ether-bond. Additionally, we have evaluated the polymer's performance toward CO_2 gas capture.

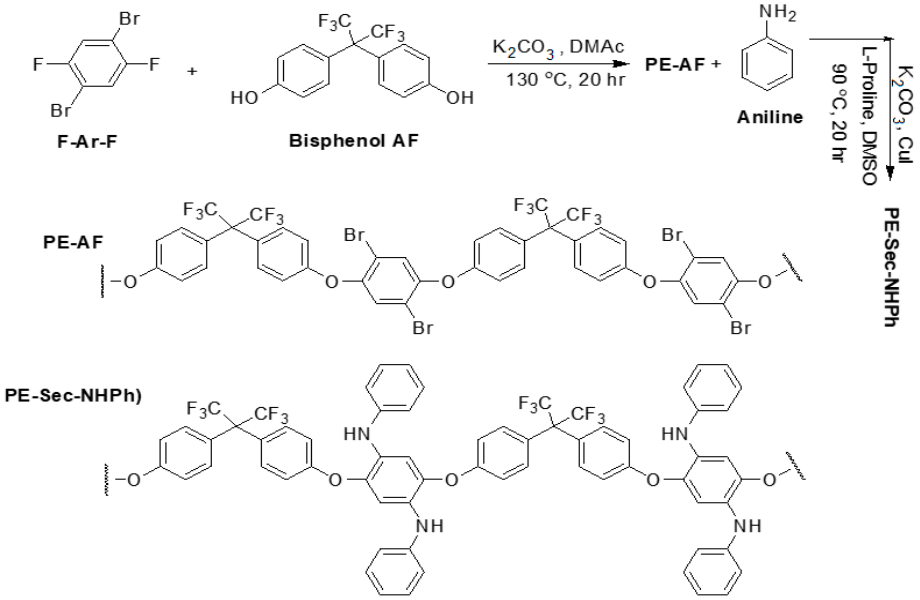
2. Results and Discussion

2.1. Synthesis and Physical Properties

An ether-based polymer with a sequence of poly(dibromobenezne-bisphenoxy hexafluoropropane)n (PE-AF) has been prepared via one-step polycondensation between 1,4-dibromo-2,5-difluorobenzene and bisphenol AF (BAF) in the presence of potassium carbonate as a base (Scheme 1). The proposed polymerization mechanism relies on the deprotonation of the bisphenol (BAF), as bis-phenoxide anion, which then attacks the para (C-F) bonds of 1,4-dibromo-2,5-difluorobenzene via a nucleophilic aromatic substitution reaction. The special para-position of the difluoro substituents assists the nucleophilic attack via the π-electrons' delocalization and reserves the aromaticity of the system. This methodology has been adopted for the preparation of several examples of polymers, where the phenoxide anion plays the role of a nucleophile and replaces the good leaving groups such as halogens and nitro groups [27–29].

After the formation of the ether linkage, the polymer was extracted as a white solid after washing the solution with 100 mL of 3% hydrochloric acid. The solid was then soaked in 100 mL water for 24 h to dissolve any potassium fluoride salt, filtered and dried at room temperature for 24 h. The final product features a pale white fluffy-textured solid with a good yield and a high solubility in common non-polar solvents such as diethyl ether and tetrahydrofuran (THF). The structural formation of the polymer was confirmed by an elemental analysis of carbon, hydrogen, oxygen, bromine and fluorine.

The post-functionalization polymerization of the parent polymer PE-AF has been demonstrated via the application of a copper-catalyzed Ullman coupling reaction. This reaction depends on the conversion of the vital C-Br bond into a C-N bond and is thus considered an amination reaction. It is achieved by following the synthetic method for the preparation of polyaminopyridines (PAPy) in the presence of copper iodide (I) and an L-proline ligand. In general, the reaction mechanism consists of oxidative addition followed by reductive elimination steps, which is well-known for most of the metal-catalyzed coupling reactions. The role of the L-Proline ligand is to maintain the copper (I) catalytic reactivity, give a high-yield product and permit the use of mild reaction conditions since the ligand-free method requires a high stoichiometric amount of the catalyst and high reaction temperature that might reach 200 °C [30–33].



Scheme 1. Molecular structures of the monomer building blocks and the polymers, PE-AF and PE-Sec-NHPh.

In this study, the new polymer PE-Sec-NHPh has been prepared via applying the Ullman coupling reaction by mixing the polymer PE-AF with aromatic aniline in the presence of copper iodide and L-proline at 90 °C. The new generated polymer is constituted by nitrogen-decorated ether-linked polymers designated as poly(aromatic-secondary amines-bisphenoxy hexafluoropropane)n, as illustrated in Scheme 1.

The polymer is formed as a pale-to-dark brown solid and is insoluble in common organic solvents such as hexane, diethyl-ether, tetrahydrofuran, chloroform, methanol, acetonitrile, N-methyl-2-pyrrolidone (NMP) and dimethylformamide (DMF) but slightly soluble in dimethylsulfoxide (DMSO) and strong polar protic solvents such as acetic and trifluoroacetic acids. The lack of solubility is related to the extended chain formation, cross-linking, π-π stacking and the higher molecular weight when compared with PE-AF. However, the higher pronounced solubility in polar protic solvents is an indication of the creation of hydrogen bonding interactions within the framework as a result of the incorporation of the secondary-amine bonds [33].

2.2. Infrared Spectroscopy (FTIR), ^{1}H-NMR, ^{13}C-NMR and Solid State ^{13}C-C-MAS

The successful formation of the polymers was confirmed by FTIR and ^{13}C-NMR (CP-MAS) (Figure 1A,B). From the FTIR, the polyether linkage (C-O-C) is confirmed by the absorption band around 1220 cm^{-1}, the disappearance of the broad OH band around 3500 cm^{-1} along with the appearance of the C-Br band at 843 cm^{-1} (Figure 1A).

Comparing the spectra of PE-AF and PE-Sec-NHPh indicated the significant disappearance of the C-Br bond at 843 cm^{-1} as an indication of the Ullman coupling reaction and the appearance of a new absorption band around 3450 cm^{-1}, which supported the inclusion of the secondary N-H bond within the polymers framework. The absorption peaks at 991, 1020 and 1000 cm^{-1} are related to the -CF_3, C-N and C-O absorption bands, respectively [7,30,31].

Moreover, the formation of a linkage (C-O-C) within the polymers was confirmed by ^{1}H- and ^{13}C-NMR. The ^{1}H-NMR data of PE-AF and PE-Sec-NHPh polymers shows two different regions of protons, (6.91–6.96, 7.62 and 6.84–7.11, 7.42), respectively, and the appearance of (160.43, 162.59 and 163.15, 165.32) peaks in ^{13}C-NMR, respectively, indicating the formation of ether linkers (C-O-C) within these polymers (Figures S1–S4 of Supplementary information).

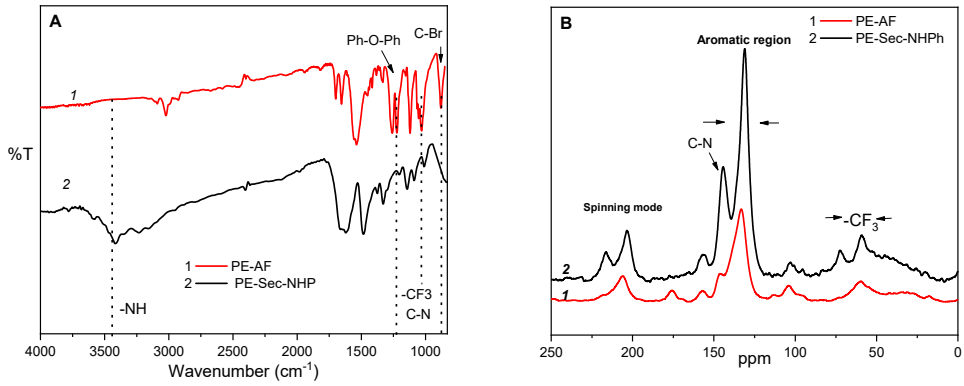


Figure 1. (**A**) IR spectra of the polymer in the range of 4000–800 cm^{-1}; (**B**) ^{13}C CP-MAS solid state of the polymers.

The solid-state ^{13}C CP-MAS NMR spectra of the polymers PE-AF and PE-Sec-NHPh have been performed for comparison purposes. Both spectra exhibit signature peaks around 65 ppm corresponding to the aliphatic -CF3 groups. On the other hand, the region at 125 to 150 ppm corresponds to the aromatic motifs and the carbon of the C-Br and C-N bonds, as shown in Figure 1B.

2.3. Scanning Electron Microscopy

The scanning electron microscopy (SEM) measurements were used to establish the phase purity of the polymers and the surface morphology changes upon polymerization. The surface of the polymer PE-AF shows a random fluffy-like texture. However, there is a notable change of the surface upon post-functionalization with the formation of random aggregated irregular spherical particles ca. 0.3–0.1 µm in size (Figure 2). This observation is consistent with the surface morphology reported for most of the amorphous organic polymers, which supports the creation of random pores and cross-linked chains within the polymers frameworks [34].

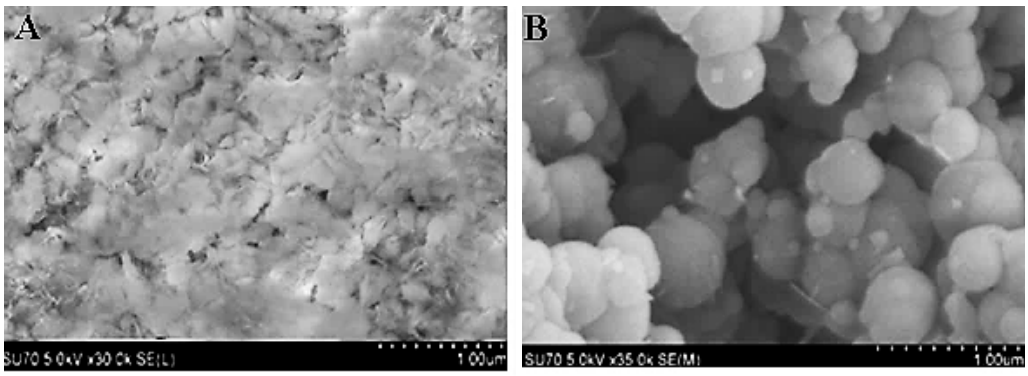


Figure 2. Scanning electron microscopy (SEM) of the polymers; (**A**) PE-AF and (**B**) PE-Sec-NHPh.

2.4. Thermal Stability

The thermal stabilities of the parent ether-linked polymer PE-AF and the post-functionalized amine-linked polymer PE-Sec-NHPh were measured up to 600 °C by using thermogravimetric analysis (TGA) at a heating rate of 10 °C/min and under nitrogen atmosphere (Figure 3A). From the TGA curves, PE-AF has shown a good thermal stability up to 300 °C with a char residue of 10%. However, upon post-functionalization, PE-Sec-NHPh reveals a higher thermal stability up to 350 °C with a higher char residue of 40%. The higher char residue of PE-Sec-NHPh is an indication of the ability of the polymer to sustain combus-

tion as determined from the limited oxygen index values (LOI) determined from the Van Krevelen correlation (VCC):

$$\text{LOI} = 17.5 + 0.4\ (\text{Char Residue})\ (\text{VCC}) \quad (1)$$

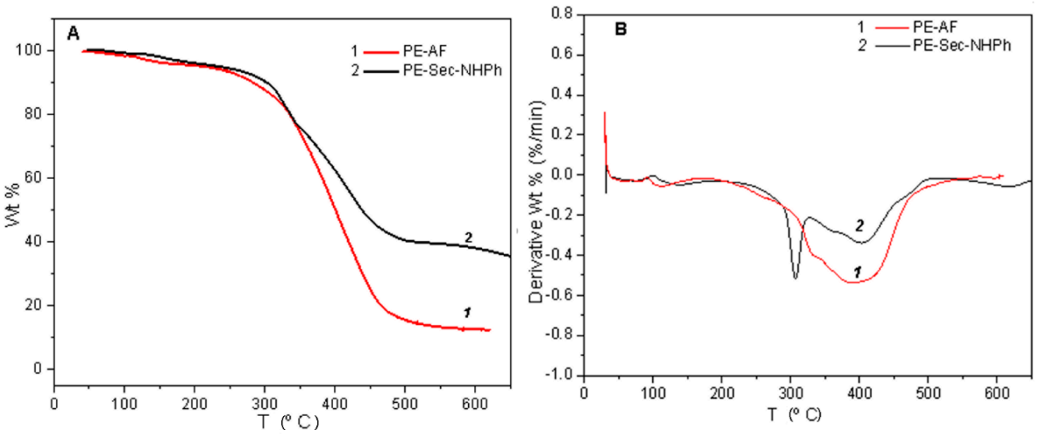


Figure 3. (**A**) TGA curves of the polymers; (**B**) DTG curves of the polymers: (1) PE-AF and (2) PE-Sec-NHPh.

When the calculated value of the LOI value is higher than 26, the polymer can be considered a flame-retardant material. According to VCC, the LOI values of PE-AF and PE-Sec-NHPh are 21.5 and 33.5, respectively. The higher LOI of PE-Sec-NHPh is attributed to the inclusion of aromatic amine, increasing the nitrogen content and thus improving the flame retardancy and the thermal stability of the polymer. This observation is consistent with the previous literature, which has shown the impact of a high nitrogen content on the thermal stability and flame-retardant property of polymers. For example, open-chain poly(amine-ethers) loaded with different numbers of nitrogen atoms have shown an outstanding stability under nitrogen atmosphere that reached 450–490 °C with a char residue of 50% [6,35]. However, the thermal stability of open-chain poly(aminopyridines) under the same conditions reached a maximum of 170 °C, which has been attributed to the impact of greater and disordered hydrogen bonding. Comparing these results shows the importance of investing more efforts into the synthesis of hybrid polymeric systems such as poly(amine-ether) for multifunctional applications [7].

From the TGA curves, the temperatures at which 50% and 100% of the polymers have decomposed are depicted in Table 1. All data have shown a higher required temperature for the decomposition of PE-Sec-NHPh when compared with PE-AF. Further investigations have determined the stages of decomposition for the polymers from their thermogravimetric derivative (DTG) curves (Figure 3B). The DTG curves of the polymers show one common degradation stage around 100 °C, which represents the loss related to the evaporation of water due to moisture. The other stages related to the degradation of the contents of polymers are one broad stage for PE-AF and two for PE-Sec-NHPh. The common degradation stage between both polymers is noted around 300 °C, which is related to the cleavage of ether-linked alkyl parts and the combustion and carbonization of the polymer backbone. The DTG peak temperature (Ts) for each stage is also mentioned in Table 1.

Table 1. Interpretation data of TGA and DTG curves.

Polymer	Stage	Ts (°C)	Wt (%)	T50% (°C)	T100% (°C)	CR%	LOI
PE-Sec-NHPh	S1: 286–326	300	10	450	470	40	33.5
	S2: 326–483	410	40				
PE-AF	S1: 250–460	400	70	400	450	10	21.5

S1, S2: First and second degradation stages; Ts: The peak temperature derived from the DTG curve; Wt %: weight loss; CR: Char residue; LOI: limited oxygen index.

2.5. Carbon Dioxide (CO_2) Adsorption

The tendency of the polymers to capture carbon dioxide gas from air constitutes one of the vital environmental applications. In this regard, porous polymers are suitable candidates for an effective capturing process on the surface and within the pores of the polymer's frameworks. In this study, since the prepared polymers PE-AF and the post-functionalized PE-Sec-NHPh are non-porous due to their one-dimensional open chain's formation, we have measured their capability for CO_2 gas adsorption on the surface. To do so, we have collected CO_2 sorption data for both polymers at 298 K and 1 atm. From the CO_2 gas uptake isotherms (Figure 4A), the gas uptake reaches (90.0 mg g^{-1}, 9.0 Wt%) and (41.0 mg g^{-1}, 4.1 Wt%) for the polymers PE-Sec-NHPh and PE-AF, respectively. This moderate uptake is attributed to the low surface area, high π-π stacking and structural collapse within the polymer's chains, which suppress the chance of CO_2-surface interactions. These results are within the range of CO_2 captured gas from moderate surface area polymers such as benzimidazole- (BILP), oxazole- (BOLP), thiazole (BTLB) and thiophene-based (TBIm) polymers under the same experimental conditions (Table 2). It is worth noting that the fact that the uptake on the PE-Sec-NHPh surface is higher by 50% when compared to PE-AF is related to the presence of nitrogen sites. It is well-known in the field of porous organic polymers that the presence of heteroatoms such as nitrogen, oxygen and nitrogen facilitates the Lewis (acid-base) interactions between the acidic CO_2 and the free lone pair of electrons of the heteroatom. Herein, the incorporation of nitrogen and oxygen within the structural framework of PE-Sec-NHPh assists this interaction and increases the gas uptake compared to PE-AF.

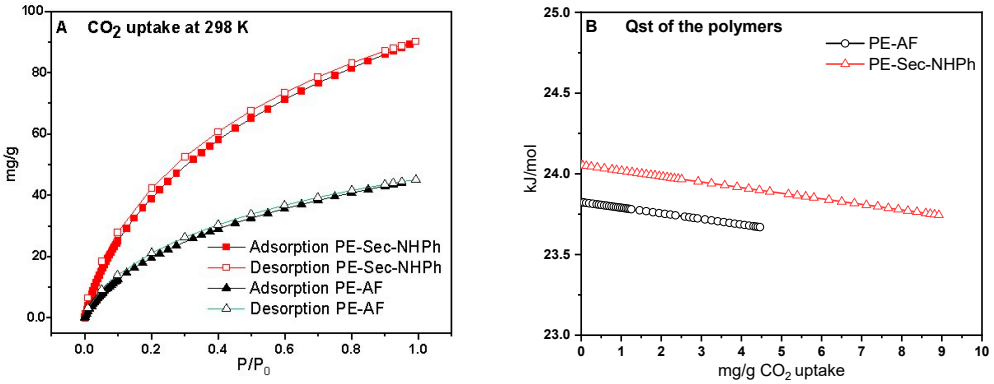


Figure 4. (**A**) CO_2 uptake at 298 K; (**B**) Binding affinity (Qst) of the loaded CO_2 gas at 298 K.

To determine the binding affinity (Qst) between CO_2 molecules and the polymer surface, we have applied the virial method of calculation by using the experimental data from the gas uptake. From the calculations, the binding affinity values are highest at zero coverage (24.2 and 23.7 kJ/mol) for PE-Sec-NHPh and PE-AF, respectively [36]. With a higher loading, these values gradually decrease, which indicates lower interactions and that the main impact is for the first layer-coverage, as shown in Figure 4B.

Interestingly, these results are consistent with the range of estimated values reported for several porous organic polymers (Table 2).

Table 2. Gas sorption properties of PE-Sec-NHPh, PE-AF and previously published polymers.

Polymer	CO_2 at 1 Bar, 298 k (mg/g)	Binding Affinity (kJ/mol)	Reference
PE-Sec-NHPh	90.0	24.2	This work
PE-AF	41.0	23.7	This work
BILP-polymers	80.7	32.0	[37]
BOLP-polymer	79.0	32.9	[38]
BTLP-polymer	87.0	29.1	[38]
TPIm-polymer	75.0	24.0	[34]

Accordingly, the findings from this section have proven the important role of the surface content in the CO_2 interactions despite the non-porous nature of the polymers [39]. However, the design of porous analogues of these polymers through the use of diamine linkers instead of aniline is in progress, as is their performance for CO_2 capture.

3. Materials and Methods

3.1. Chemicals and Characterization Methods

All chemicals were purchased from the Sigma-Aldrich supplier (Taufkirchen, Germany) and used without further purification, unless otherwise mentioned. The polymer synthesis and the post-functionalization were performed under nitrogen atmosphere using the Schlenk line technique. Carbon, hydrogen, oxygen, bromine and nitrogen analyses were performed using a Vario EL elemental analyzer (EL cube-model, Haan, Germany). ^{13}C-NMR CP-MAS Solid-state NMR measurements were performed at 9.4 Tesla on a Bruker Avance 400 spectrometer (Mundelein, IL, USA). The thermogravimetric analysis (TGA) was carried out using TA Instruments Q-5000IR series thermal gravimetric analyzer (New Castle, DE, USA) under nitrogen atmosphere (heating rate 10 °C/min). For Scanning Electron Microscopy Imaging (SEM), the sample was prepared by dispersing the material onto a sticky carbon surface attached to a flat aluminum sample holder. Under nitrogen atmosphere, the sample was then coated with platinum at 1×10^{-5} mbar of pressure for 90 s before imaging. Images were taken on a Hitachi SU-70 Scanning Electron Microscope (Dallas, TX, USA). IR spectra were recorded on a Shimadzu FT-IR-8300 (Corston, UK) on KBr pellets in the wavenumber range 4000–400 cm^{-1}. Carbon dioxide uptake was obtained by using a TriStar II 3020 surface area and porosity analyzer (Micromeritics, Norcross, GA, USA). The adsorption of CO_2 onto polymers was studied using CO_2 as a working gas at 298 K. The sample was preliminarily degassed at 120 °C for 12 h under helium flow. Adsorption is measured under isothermal conditions in a thermostated system at 298 K. The concentration of CO_2 in the outlet gas is measured by a detector device.

3.2. Synthesis of Bromo-Substituted Ether-Based Polymer (PE-AF)

The polycondensation polymerization between 1,4-dibromo-2,5-difluorobenzene (F-Ar-F) and 2,2-bis(4-hydroxyphenyl) hexafluoropropane (Bisphenol AF or BAF) was carried out in one-pot polymerization. To a solution of F-Ar-F (1.6 mmol) and BAF derivative (1.6 mmol) in (15 mL) dimethylacetamide (DMAc), potassium carbonate (4 mmol) was added, and the solution was allowed to warm up to 130 °C for 20 h under nitrogen flow. After the polymerization, the product was poured into 100 mL of 3% hydrochloric acid, and the polymer was precipitated as a white solid with a 77% yield and dried under vacuum at room temperature for 24 h. ^{1}H NMR (500 MHz, DMSO-d^{6}, ppm, 298 k): δ (6.91–6.96) (m, ^{2}H, Ar-H), 7.62 (s, ^{1}H, Ar-H), ^{13}C NMR (500 MHz, DMSO-d^{6}, ppm, 298 k): δ 116.48, 131.28, 135.21, 142.54, 148.12, 160.43, 162.59 (Ar-C), 39.92 (methylene-C), 52.3 (-CF3). The physical appearance and percent composition of the prepared polymer are summarized in Table 3.

Table 3. Summarized physical appearance and percent composition of the polymers.

Polymer */Formula $(Monomer)_n$	FW ‖ (g/mol)	Appearance	Yield (%)	Elemental Analyses Calculated (Found) (Wt%)				
				C	**H**	**Br**	**O**	**F** ‡
(PE-AF)	552.1	White solid	77.0	45.68 (45.62)	1.83 (2.00)	28.95 (28.33)	2.90 (2.78)	20.65 (20.62)
				C	**H**	**N**	**O**	**F**
(PE-Sec-NHPh)	576.54	Pale brown solid	85.0	68.75 (68.11)	3.85 (3.55)	4.86 (4.76)	2.78 (2.67)	19.77 20.91

* Polymer abbreviation, ‖ FW: the molecular weight of one repeating unit, ‡ F: calculated (Expected).

3.3. Synthesis of Aniline-Substituted Ether-Based Polymer (PE-Sec-NHPh)

The post-functionalization of the polymer (PE-AF) was performed by applying the Ullmann coupling reaction between the bromo-substituents of the polymer (PE-AF) (5 mmol), and a mixture of aniline (7.5 mmol), potassium carbonate (10 mmol), copper iodide (0.5 mmol) and L-proline (1 mmol) in 10 mL dimethyl sulfoxide (DMSO). The mixture was heated up to 90 °C for 24 h under nitrogen flow. The cooled mixture was partitioned between water and ethyl acetate. The final solid product was filtered and washed several times with water, 0.1M HCl, 0.1M NaOH and acetone and finally dried under vacuum at room temperature for 24 h. ^{1}H NMR (500 MHz, DMSO-d^6, ppm, 298 k): δ (6.86–7.24) (m, Ar-H), 7.41 (s, Ar-H), 4.69 (s, NH) ^{13}C NMR (500 MHz, DMSO-d^6, ppm, 298 k): δ 118.4, 121.3, 129.4, 130.7, 132.1, 142.8, 144.5, 148.6, 160.7, 165.7 (Ar-C), 40.22 (methylene-C), 55.2 (-CF_3). The physical appearance and percent composition of the prepared polymer are summarized in Table 3.

4. Conclusions

In this report, the synthesis of an ether-linked polymer via a nucleophilic substitution reaction on the C-F bond of substituted and fluorinated benzene and its post-functionalized analogue was achieved by applying the Ullman coupling reaction. The polymers revealed varied properties, indicating the significant role of the post-functionalization reaction and the inclusion of the aniline moiety. Notable improvements were confirmed, including the rigidity, thermal stability and surface morphology of PE-Sec-NHPh over PE-AF. The polymer PE-Sec-NHPh has a thermal stability up to 350 °C and a defined particle size. Furthermore, the polymer PE-Sec-NHPh has shown an enhanced capability for carbon-dioxide uptake upon the incorporation of the nitrogen content in the polymer structure. We are working on the application of the Ullman coupling of diamine linkers for the creation of porous organic polymers, which are vital for environmental applications.

Supplementary Materials: The following supporting information can be downloaded at: https://www.mdpi.com/article/10.3390/separations9030055/s1. Figure S1: ^{1}H-NMR of PE-AF in DMSO-d^6; Figure S2: ^{13}C-NMR of PE-AF in DMSO-d^6; Figure S3: ^{1}H-NMR of PE-Sec-NHPh in DMSO-d^6; Figure S4: ^{13}C-NMR of PE-Sec-NHPh in DMSO-d^6.

Author Contributions: Conceptualization, T.M.A.A.-S. and S.S.A.-T.; methodology, S.S.A.-T.; software, T.S.A.; validation, T.M.A.J., T.M.A.A.-S. and S.S.A.-T.; formal analysis, T.M.A.J.; investigation, T.S.A.; resources, S.S.A.-T. and T.M.A.A.-S.; data curation, T.M.A.A.-S.; writing—original draft preparation, S.S.A.-T. and T.M.A.A.-S.; writing—review and editing, T.S.A. and T.M.A.J.; visualization, T.M.A.A.-S.; supervision, S.S.A.-T.; project administration, S.S.A.-T. and T.M.A.A.-S.; funding acquisition, S.S.A.-T. All authors have read and agreed to the published version of the manuscript.

Funding: This research was funded by Tafila Technical University, grant number 122/2020.

Institutional Review Board Statement: Not applicable.

Informed Consent Statement: Not applicable.

Data Availability Statement: Not applicable.

Acknowledgments: The authors gratefully acknowledge the water, environment and arid regions research center at Al Al–Bayt University, Jordan for the polymers' characterizations.

Conflicts of Interest: The authors declare no conflict of interest. The funders had no role in the design of the study; in the collection, analyses, or interpretation of data; in the writing of the manuscript, or in the decision to publish the results.

Sample Availability: Samples of the compounds are not available from the authors.

References

1. Bricaud, Q.; Cravino, A.; Leriche, P.; Roncali, J. Terthiophene-cyanovinylene π-conjugated polymers as donor material for organic solar cells. *Synthmet* **2009**, *159*, 2534–2538. [CrossRef]
2. Tan, M.; Sum, Y.; Ying, J.; Zhang, Y. A mesoporous poly-melamine-formaldehyde polymer as a solid sorbent for toxic metal removal. *Energy Environ. Sci.* **2013**, *6*, 3254–3259. [CrossRef]
3. Jung, J.; Jo, J.; Chueh, C.; Liu, F.; Jo, W.; Russell, T.; Jen, A. Fluoro-Substituted n-Type Conjugated Polymers for Additive-Free All-Polymer Bulk Heterojunction Solar Cells with High Power Conversion Efficiency of 6.71%. *Adv. Mater.* **2015**, *27*, 3310–3317. [CrossRef]
4. Bourbigot, S.; Duquesne, S. Fire retardant polymers: Recent developments and opportunities. *J. Mater. Chem.* **2007**, *17*, 2283–2300. [CrossRef]
5. Qi, Y.; Wang, J.; Kou, Y.; Pang, H.; Zhang, S.; Li, N.; Liu, C.; Weng, Z.; Jian, X. Enabling low voltage losses and high photocurrent in fullerene-free organic photovoltaics. *Nat. Commun.* **2019**, *10*, 570.
6. Liu, B.; Hu, W.; Chen, C.; Jiang, Z.; Zhang, W.; Wu, Z.; Matsumoto, T. Soluble aromatic poly(ether ketone)s with a pendant 3,5-ditrifluoromethylphenyl group. *Polymer* **2004**, *45*, 3241–3247. [CrossRef]
7. Chang, G.-J.; Xu, Z.; Lin, R.-X.; Luo, X. Synthesis and Properties of Novel Poly(amine ether)s. *Chin. J. Chem.* **2007**, *25*, 1207–1211. [CrossRef]
8. Hemvichian, K.; Ishida, H. Thermal decomposition processes in aromatic amine-based polybenzoxazines investigated by TGA and GC–MS. *Polymer* **2002**, *43*, 4391–4402. [CrossRef]
9. Vasanthi, B.J.; Ravikumar, L. Synthesis and Characterization of Poly(azomethine ester)s with a Pendent Dimethoxy Benzylidene Group. *Open. J. Pol. Chem.* **2013**, *3*, 70–77. [CrossRef]
10. Wang, C.; Shieh, S.; LeGoff, E.; Kanatzidis, M.G. Synthesis and Characterization of a New Conjugated Aromatic Poly(azomethine) Derivative Based on the 3′, 4′-Dibutyl-α-Terthiophene Building Block. *Macromolecules* **1996**, *29*, 3147–3156. [CrossRef]
11. Mihai, I.; Ivanoiu, M.; Stafie, L.V.; Grigoras, M. Suzuki polycondensation: A simple way for synthesis of new polyazines containing thiophene and fluorene moieties. *e-Polymers* **2011**, *31*, 1–10. [CrossRef]
12. Zhao, J.; Gong, C.; Zhang, S.; Shao, Y.; Li, Y. Synthesis of a new pyridine-containing diamine and related polyimide. *Chin. Chem. Lett.* **2010**, *21*, 277–278. [CrossRef]
13. Rai, S.; Bajpai, A.; Lokhandwal, S. Condensation Polymers of Terephthalic Acid and 1,4-Diaminobutane and Their Schiff Base Complexes. *J. Polym.* **2013**, *2013*, 278576. [CrossRef]
14. Tabish, A.; Varghese, A.M.; Wahab, M.A.; Karanikolos, G.N. Perovskites in the energy grid and CO_2 conversion: Current context and future directions. *Catalysts* **2020**, *10*, 95. [CrossRef]
15. Varghese, A.; Mittal, V. *Performance of Various Adsorbents Towards Diverse Gases: A Comparative Study, Functional Nanomaterials and Nanotechnologies: Applications for Energy & Environment*; Central West Publishing: Orange, NSW, Australia, 2018; pp. 305–404.
16. Varghese, A.M.; Reddy, K.S.K.; Singh, S.; Karanikolos, G.N. Performance enhancement of CO_2 capture adsorbents by UV treatment: The case of self-supported graphene oxide foam. *Chem. Eng. J.* **2020**, *386*, 124022. [CrossRef]
17. Olivares-Marín, M.; Maroto-Valer, M.M. Development of adsorbents for CO_2 capture from waste materials: A review. *Greenh. Gases Sci. Technol.* **2012**, *2*, 20–35. [CrossRef]
18. Wang, Q.; Luo, J.; Zhong, Z.; Borgna, A. CO_2 capture by solid adsorbents and their applications: Current status and new trends. *Energy Environ. Sci.* **2011**, *4*, 42–55. [CrossRef]
19. Dzubak, A.L.; Lin, L.C.; Kim, J.; Swisher, J.A.; Poloni, R.; Maximoff, S.N.; Smit, B.; Gagliardi, L. Ab initio carbon capture in open-site metal–organic frameworks. *Nat. Chem.* **2012**, *4*, 810–816. [CrossRef]
20. Favvas, E.P.; Heliopoulos, N.S.; Karousos, D.S.; Devlin, E.; Papageorgiou, S.K.; Petridis, D.; Karanikolos, G.N. Mixed matrix polymeric and carbon hollow fiber membranes with magnetic iron-based nanoparticles and their application in gas mixture separation. *Mat. Chem. Phys.* **2019**, *223*, 220–229. [CrossRef]
21. Iqbal, N.; Wang, X.; Yu, J.; Jabeen, N.; Ullah, H.; Ding, B. In situ synthesis of carbon nanotube doped metal–organic frameworks for CO_2 capture. *RSC Adv.* **2016**, *6*, 4382–4386. [CrossRef]
22. Labropoulos, A.; Veziri, C.; Kapsi, M.; Pilatos, G.; Likodimos, V.; Tsapatsis, M.; Kanellopoulos, N.K.; Romanos, G.E.; Karanikolos, G.N. Carbon nanotube selective membranes with subnanometer, vertically aligned pores, and enhanced gas transport properties. *Chem. Mater.* **2015**, *27*, 8198–8210. [CrossRef]
23. Perdikaki, A.V.; Labropoulos, A.I.; Siranidi, E.; Karatasios, I.; Kanellopoulos, N.; Boukos, N.; Falaras, P.; Karanikolos, G.N.; Romanos, G.E. Efficient CO oxidation in an ionic liquid-modified, Au nanoparticle-loaded membrane contactor. *Chem. Eng. J.* **2016**, *305*, 79–91. [CrossRef]

24. Rao, A.B.; Rubin, E.S. Identifying cost-effective CO_2 control levels for amine-based CO_2 capture systems. *Ind. Eng. Chem. Res.* **2006**, *45*, 2421–2429. [CrossRef]
25. Tzialla, O.; Veziri, C.; Papatryfon, X.; Beltsios, K.; Labropoulos, A.; Iliev, B.; Adamova, G.; Schubert, T.; Kroon, M.; Francisco, M. Zeolite imidazolate framework-ionic liquid hybrid membranes for highly selective CO_2 separation. *J. Phys. Chem. C* **2013**, *117*, 18434–18440. [CrossRef]
26. Zainab, G.; Iqbal, N.; Babar, A.A.; Huang, C.; Wang, X.; Yu, J.; Ding, B. Freestanding, spider-web-like polyamide/carbon nanotube composite nanofibrous membrane impregnated with polyethyleneimine for CO_2 capture. *Compos. Commun.* **2017**, *6*, 41–47. [CrossRef]
27. Irvin, J.; Neef, C.; Kane, K.; Cassidy, P.; Tullos, G.; Clair, A.J. Polyethers derived from bisphenols and highly fluorinated aromatics. *Polym. Sci. Part A Polym. Chem.* **1992**, *30*, 1675–1679. [CrossRef]
28. Tkachenko, I.; Kurioz, Y.; Kovalchuk, A.; Kobzar, Y.; Shekera, O.; Tereshchenko, O.; Nazarenko, V.; Shevchenko, V. Optical properties of azo-based poly(azomethine)s with aromatic fluorinated fragments, ether linkages and aliphatic units in the backbone. *Mol. Cryst. Liq. Cryst.* **2020**, *697*, 85–96. [CrossRef]
29. Chen, S.; Ren, D.; Li, B.; Li, K.; Chen, L.; Xu, M.; Liu, X. Benzoxazine Containing Fluorinated Aromatic Ether Nitrile Linkage: Preparation, Curing Kinetics and Dielectric Properties. *Polymers* **2019**, *11*, 1036. [CrossRef]
30. Puthiaraj, P.; Ahn, W. Ullmann coupling of aryl chlorides in water catalyzed by palladium nanoparticles supported on amine-grafted porous aromatic polymer. *Mol. Catal.* **2017**, *437*, 73–79. [CrossRef]
31. Reis, L.; Ligiéro, C.; Andrade, A.; Taylor, J.; Miranda, P. Preparation of Polyaminopyridines Using a CuI/l-Proline-Catalyzed C-N Polycoupling Reaction. *Materials* **2012**, *5*, 2176–2189. [CrossRef]
32. Ma, D.; Cai, Q. L-Proline Promoted Ullmann-Type Coupling Reactions of Aryl Iodides with Indoles, Pyrroles, Imidazoles or Pyrazoles. *Synletter* **2004**, *1*, 128–130. [CrossRef]
33. Quivelli, A.; Vitale, P.; Perna, F.; Capriati, V. Reshaping Ullmann Amine Synthesis in Deep Eutectic Solvents: A Mild Approach for Cu-Catalyzed C–N Coupling Reactions with No Additional Ligands. *Front. Chem.* **2019**, *7*, 723. [CrossRef] [PubMed]
34. Altarawneh, S.; Ababneh, T.; Al-Momani, L.; Aljaafreh, I. New Microporous Thiophene-Pyridine Functionalized Imine-Linked Polymer for Carbon-Dioxide Capture. *Polym. Sci. Ser. B* **2018**, *60*, 789–797. [CrossRef]
35. Alves, W.; Malmonge, J.; Mattoso, L.; De Medeiros, E. Non-isothermal decomposition kinetics of conductive polyaniline and its derivatives. *Polimeros* **2018**, *28*, 285–292. [CrossRef]
36. Gus'Kov, V.; Kudasheva, F.; Bogolyuk, G. Second virial coefficients of adsorption isotherms of organic molecules on porous polymers. *Russ. J. Phys. Chem. A* **2013**, *87*, 879–881. [CrossRef]
37. Altarawneh, S.; İslamoğlu, T.; Sekizkardes, A.; El-Kaderi, H. Effect of Acid-Catalyzed Formation Rates of Benzimidazole-Linked Polymers on Porosity and Selective CO_2 Capture from Gas Mixtures. *Environ. Sci. Technol.* **2015**, *49*, 4715–4723. [CrossRef]
38. Rabbani, M.; Islamoglu, T.; El-Kaderi, H. Benzothiazole- and Benzoxazole-Linked Porous Polymers for Carbon Dioxide Storage and Separation. *J. Mater. Chem. A* **2017**, *5*, 258–264. [CrossRef]
39. Varghese, A.; Karanikolos, G. CO_2 capture adsorbents functionalized by amine–Bearing polymers: A. review. *Int. J. Greenh. Gas Control* **2020**, *96*, 103005. [CrossRef]